Multidim Syst Sign Process (2010) 21:197–211
DOI 10.1007/s11045-009-0097-0

Fractal capacity dimension of three-dimensional histogram from color images

Julien Chauveau · David Rousseau · François Chapeau-Blondeau

Received: 26 March 2009 / Revised: 1 July 2009 / Accepted: 8 December 2009 /
Published online: 22 December 2009

Abstract To contribute to the important task of characterizing the complex multidimensional structure of natural images, a fractal characterization is proposed for the colorimetric organization of natural color images. This is realized from their three-dimensional RGB color histogram, by applying a box-counting procedure to assess the dimensionality of its support. Regular scaling emerges, almost linear over the whole range of accessible scales, and with non-integer slope in log-log allowing the definition of a capacity dimension for the histogram. This manifests a fractal colorimetric organization with a self-similar structure of the color palette typically composing natural images. Such a fractal characterization complements other previously known fractal properties of natural images, some reported recently in their colorimetric organization, and others reported more classically in their spatial organization. Such fractal multiscale features uncovered in natural images provide helpful clues relevant to image modeling, processing and visual perception.

Keywords Color images · Three-dimensional histogram · Scaling · Fractal dimension · Multicomponent images

1 Introduction

Natural images are complex multidimensional information-carrying signals. Their understanding and modeling are essential to many tasks in image processing and vision, and advances are still needed in this direction. Among specific properties that have been found constitutive of the complex structure of natural images are fractal properties. Principally, fractal or self-similarity or scaling properties have been observed in the spatial organization of natural images (Ruderman and Bialek 1994; Ruderman 1997; Hsiao and Millane 2005). Such spatial fractal properties can be related to the many features and details which

J. Chauveau · D. Rousseau · F. Chapeau-Blondeau (✉)
Laboratoire d'Ingénierie des Systèmes Automatisés (LISA), Université d'Angers,
62 avenue Notre Dame du Lac, 49000 Angers, France
e-mail: chapeau@univ-angers.fr

usually exist across many spatial scales, in a self-similar way, in natural scenes. Such fractal self-similar structures have also been found to extend to the temporal organization of time-varying sequences of natural images, as perceived by the visual system (Dong and Atick 1995). These findings of such spatial or temporal fractal scaling properties are helpful to construct more realistic models for natural images, and carry relevance for image coding and processing (Pesquet-Popescu and Lévy Véhel 2002; Srivastava et al. 2003; Chen et al. 2008) and vision systems (Knill et al. 1990; Olshausen and Field 2000).

In the present paper, we will address another, complementary, aspect of the fractal properties of natural images. Beyond the spatial and temporal organizations of natural images, we address here their colorimetric organization. Some evidence has recently been reported that a fractal or self-similar organization also exists in the colorimetric domain for natural images (Chauveau et al. 2008; Chapeau-Blondeau et al. 2009). The pixels of natural color images would tend to distribute, over the colorimetric space, in a self-similar fractal arrangement. This has been shown in Chauveau et al. (2008), Chapeau-Blondeau et al. (2009) by means of the evaluation of the correlation dimension of the distribution of pixels in the colorimetric space, as represented by the three-dimensional color histogram of the images. Two distinct estimators in Chauveau et al. (2008) and in Chapeau-Blondeau et al. (2009) have been tested for the correlation dimension, which confirm the presence of non-integer correlation dimension manifesting a fractal distribution of the pixels in the colorimetric space. We complement these investigations here by considering another approach to further characterize a fractal colorimetric organization. We evaluate the capacity dimension of the three-dimensional histogram of color images. Such a capacity dimension characterizes the structure of the support of the three-dimensional histogram, which expresses, in the colorimetric space, which colors are present in an image and which are not. In other words, the capacity dimension characterizes the structure of the color palette employed by Nature to compose a given natural image. We show here that such a color palette tends to display a fractal organization, identified by a non-integer capacity dimension. By contrast, the correlation dimension of Chauveau et al. (2008), Chapeau-Blondeau et al. (2009) offers a more composite view, as it simultaneously characterizes the color palette and the populations of pixels distributing among these existing colors. These are two complementary approaches on the fractal colorimetric organization of images, which are made possible by the evaluation of the capacity dimension we perform here.

2 Three-dimensional color histogram

We consider RGB color images (Sharma 2003), with each component R red, G green and B blue varying among Q possible integer values in $[0,\ Q-1]$ at each pixel of spatial coordinate (x_1, x_2). The histogram of such color images is a three-dimensional structure comprising Q^3 colorimetric cells, each of which containing the pixels with this color in the image. For the very common choice $Q = 2^8 = 256$, the histogram with its $Q^3 = 2^{24} \approx 16.8 \times 10^6$ cells is a large data structure which can display complex organization. Instead of the full three-dimensional histogram, three marginal one-dimensional histograms, separately for each R, G or B component, are often considered to lead to simpler data handling. In addition, the full three-dimensional histogram can be highly nonuniform. For a typical RGB color image with size 512×512 and $Q = 256$, a total of $512^2 = 2^{18}$ pixels distribute among the $Q^3 = 2^{24}$ colorimetric cells. This means that in the three-dimensional color histogram, most of the cells are likely to be empty, while cells corresponding to dominant colors in the image may be highly populated. A typical three-dimensional color histogram is thus a large data structure,

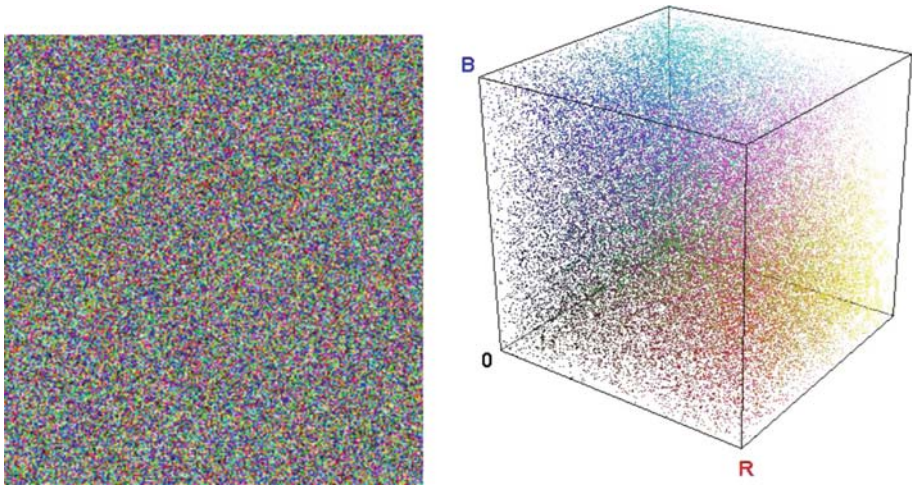

Fig. 1 Random RGB color image $\boldsymbol{I_3}(x_1, x_2)$ of size 512 × 512 pixels (*left*) and its three-dimensional histogram in the colorimetric cube $[0,\ Q-1=255]^3$ as a three-dimensional manifold (*right*)

highly nonuniform, with possibly large voids, some high local concentrations of pixels, an overall diffuse character, and not so often considered (in place of the three marginal histograms). Such features can be perceived on the two examples of three-dimensional color histograms from natural images shown in Fig. 7. We will implement here a characterization of the three-dimensional color histogram, manifesting the prevalence of a fractal organization.

3 Fractal characterization

RGB color images have been tested for their fractal organization by applying a box-counting procedure as follows. The colorimetric cube $[0,\ Q-1]^3$ is successively covered with boxes of side a and volume a^3, with varying a. For each box size a, one computes the number $N(a)$ of boxes which are needed to cover the support of the three-dimensional histogram, i.e. to cover all the cells of the colorimetric cube which are occupied by pixels of the image.

For calibration purpose, we apply first this measuring process on reference RGB images with known properties for their three-dimensional histogram. We consider a random image $\boldsymbol{I_3}(x_1, x_2)$ for which each color component R, G or B is uniformly drawn at random in $[0, 255]$ independently at each pixel (x_1, x_2). Such a color image $\boldsymbol{I_3}(x_1, x_2)$ is endowed with a three-dimensional histogram where the pixels uniformly distribute over the colorimetric cube $[0,\ Q-1=255]^3$, as shown in Fig. 1.

In a similar way, we also consider a random image $\boldsymbol{I_2}(x_1, x_2)$ for which the two components R and G are uniformly drawn at random in $[0, 255]$ independently at each pixel (x_1, x_2). In addition, the B component is fixed everywhere to the constant value 128. Such a color image $\boldsymbol{I_2}(x_1, x_2)$ is endowed with a three-dimensional histogram which reduces to a two-dimensional manifold: the pixels uniformly distribute over the plane with equation $B = 128$ in the colorimetric cube $[0,\ Q-1=255]^3$, as shown in Fig. 2.

Finally we introduce a random image $\boldsymbol{I_1}(x_1, x_2)$ for which the component R is uniformly drawn at random in $[0, 255]$ independently at each pixel (x_1, x_2). In addition, the remaining G and B components are determined according to the value of the R component as $G = R$

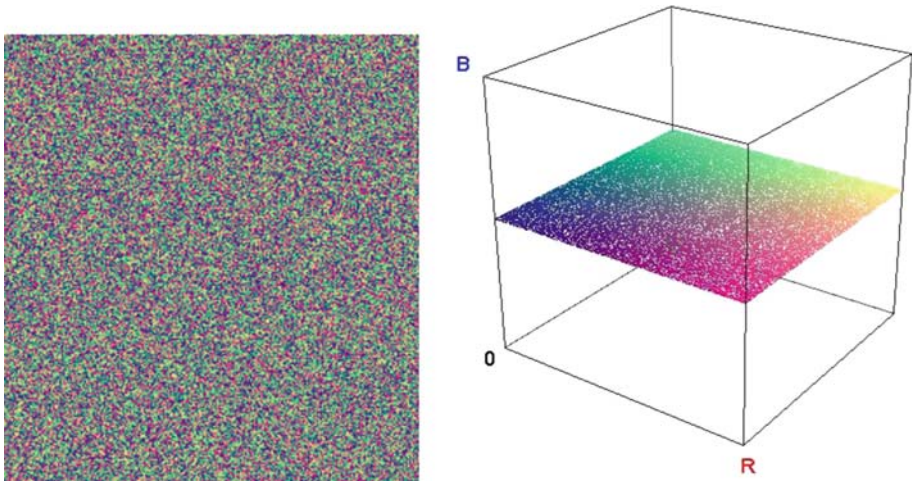

Fig. 2 Random RGB color image $\boldsymbol{I_2}(x_1, x_2)$ of size 512×512 pixels (*left*) and its three-dimensional histogram in the colorimetric cube $[0,\ Q-1=255]^3$ as a two-dimensional manifold (*right*)

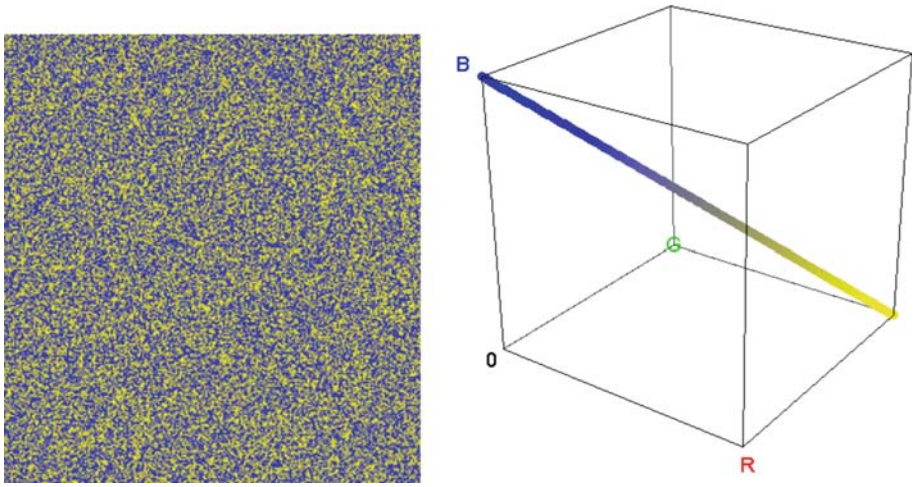

Fig. 3 Random RGB color image $\boldsymbol{I_1}(x_1, x_2)$ of size 512×512 pixels (*left*) and its three-dimensional histogram in the colorimetric cube $[0,\ Q-1=255]^3$ as a one-dimensional manifold (*right*)

and $B = 255 - R$ at each pixel (x_1, x_2). Such a color image $\boldsymbol{I_1}(x_1, x_2)$ is endowed with a three-dimensional histogram which reduces to a one-dimensional manifold: the pixels uniformly distribute over the diagonal with equation $(G = R,\ B = 255 - R)$ in the colorimetric cube $[0,\ Q-1=255]^3$, as shown in Fig. 3.

For each three-dimensional histogram of reference shown in Figs. 1–3, we count the number $N(a)$ of covering boxes at scale a.[1] For the histogram which is a one-dimensional

[1] In the plots like Fig. 4, non-integer values of the box size a correspond to the cubic root of the volume of boxes of the form $b \times b \times b/2$ or $b \times b/2 \times b/2$ with b a power of 2. The corresponding count $N(a)$ results from an average over the three possible configurations of such boxes relative to the three coordinate axes (R, G, B).

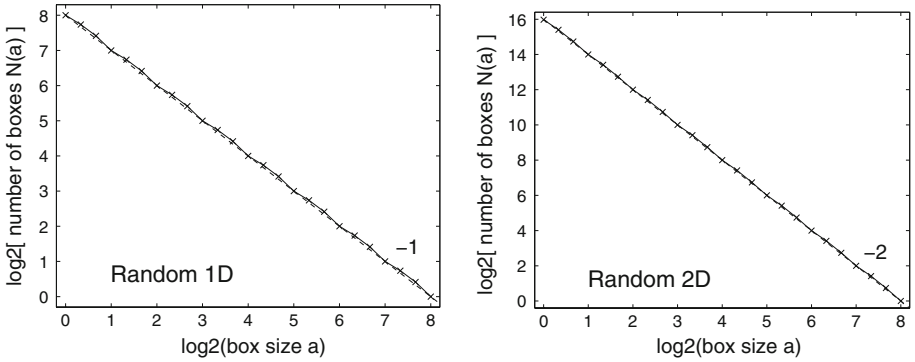

Fig. 4 Number $N(a)$ of covering boxes with size a to cover the three-dimensional histogram of image $\boldsymbol{I_1}(x_1, x_2)$ from Fig. 3 (*left*), and image $\boldsymbol{I_2}(x_1, x_2)$ from Fig. 2 (*right*). *Dotted lines* show the slopes -1 (*left*) and -2 (*right*)

manifold in Fig. 3, the count $N(a)$ is expected to follow a simple power law $N(a) \propto a^{-D}$ with an exponent $D = 1$. This is verified in Fig. 4. For the histogram which is a two-dimensional manifold in Fig. 2, the count $N(a)$ is expected to follow a power law $N(a) \propto a^{-D}$ with $D = 2$. This is also verified in Fig. 4.

For the histogram in Fig. 1 where the pixels uniformly distribute over the whole colorimetric cube $[0, Q-1 = 255]^3$, the count $N(a)$ is expected to follow a power law $N(a) \propto a^{-D}$ with $D = 3$. This is verified in Fig. 5 only at large scales a. At the smallest scale $a = 1$, the straight line with slope -3 in log-log figuring the power law $N(a) \propto a^{-3}$ in Fig. 5, points to a count $N(a = 1) = 2^{24}$ which precisely matches the total number of colorimetric cells in the colorimetric cube $[0, Q-1 = 255]^3$. However, the original image $\boldsymbol{I_3}(x_1, x_2)$ of Fig. 1 contains only a total of $N_{\text{pix}} = 512 \times 512 = 2^{18}$ pixels. Therefore at scale $a = 1$, a total number of 2^{18} boxes of size a is sufficient to cover all the occupied cells of the three-dimensional histogram in Fig. 1. Clearly, if only $N_{\text{pix}} = 2^{18}$ pixels uniformly distribute among 2^{24} colorimetric cells, there will be no more than 2^{18} occupied cells, as seen in Fig. 5. In this way, as the box size a is reduced, if the power law $\propto a^{-D}$ predicts a number of occupied boxes larger than the total number N_{pix} of pixels in the image, the experimental count $N(a)$ of occupied boxes will deviate from the power law to saturate as it cannot exceed N_{pix}. It is important to realize this possibility of saturation of the number of covering boxes $N(a)$ at small scales a, which will saturate in practice according to the total number of pixels N_{pix} in the image, and may therefore deviate from an underlying power law $N(a) \propto a^{-D}$ at small scales a due to the limited number of observed pixels. This possibility will be relevant to interpret the observations on natural images to come next.

A final random test image $\boldsymbol{I_g}(x_1, x_2)$ was generated with, at each pixel (x_1, x_2), the value of each component R, G and B selected independently from a Gaussian probability density with mean 128 and standard deviation 256/6, and then clipped into $[0, 255]$. This Gaussian random image $\boldsymbol{I_g}(x_1, x_2)$ is also characterized by a compact distribution of the colors in the colorimetric cube $[0, 255]^3$. This is associated in Fig. 5 for $\boldsymbol{I_g}(x_1, x_2)$, with a number of covering boxes $N(a) \propto a^{-D}$ with $D = 3$, as shown by the log-log plot matching a straight line with slope -3, at least at large scales a, and with a similar saturation as for $\boldsymbol{I_3}(x_1, x_2)$, at small scales a, due to the limited number of pixels.

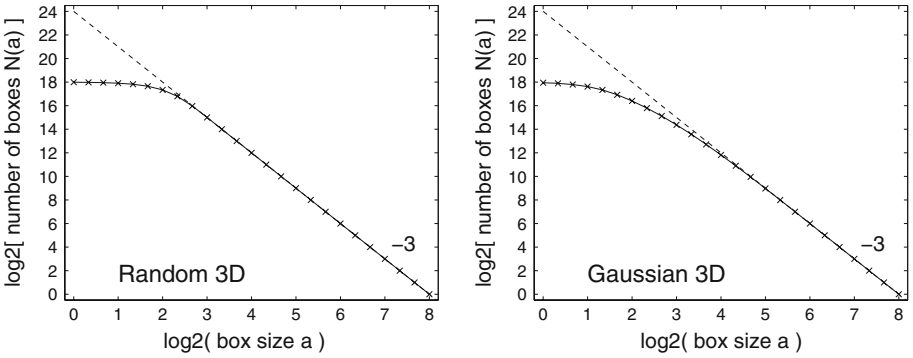

Fig. 5 Number $N(a)$ of covering boxes with size a to cover the three-dimensional histogram of uniform random image $\boldsymbol{I_3}(x_1, x_2)$ from Fig. 1 (*left*), and a Gaussian random image $\boldsymbol{I_g}(x_1, x_2)$ (*right*). *Dotted lines* show the slope -3

4 Natural color images

We now apply the box-counting procedure of Sect. 3 to characterize the three-dimensional histogram of natural color images. We have considered various common RGB color images, with size $N = 512 \times 512$ pixels and $Q = 256$ levels. Examples of such images are shown in Fig. 6, with two typical three-dimensional color histograms depicted in Fig. 7.

For the images of Fig. 6, log-log plots of the number $N(a)$ of covering boxes are presented in Fig. 8.

The remarkable observation in Fig. 8 is that the plots of $\log[N(a)]$ versus $\log(a)$ are well approximated by straight lines with slope $-D$, over a significant range of scales a. This is equivalent to a number $N(a)$ of covering boxes following a power law $N(a) \propto a^{-D}$, and with the exponent D from Fig. 8 which tends to assume non-integer values significantly below 3. At small scales a, there is usually a departure from the power law $N(a) \propto a^{-D}$ which can be related to the finite number of pixels present in the images, which limits the total count of boxes $N(a)$, as explained at the end of Sect. 3. This saturation of $N(a)$ is image-dependent since at the smallest scale $a = 1$, the number of covering boxes $N(a = 1)$ saturates exactly at the number of distinct colors present in the image.

The results of Fig. 8 manifesting a power law $N(a) \propto a^{-D}$ are typical of the behavior that was observed while testing many natural color images, with an exponent D that was found to vary between 2.2 and 2.5 typically for natural images. This type of behavior, with non-integer exponent D, identifies what can be viewed as a fractal organization of the colors present in natural images. The box covering procedure as used here, characterizes the structure of the support of the three-dimensional histogram of color images. It shows how the color that are present in the images distribute across the colorimetric cube, according to the colorimetric scale, for close neighboring colors or far apart distant colors. Alternatively, the measure of Fig. 8 characterizes the regions of the colorimetric cube that contribute in providing colors that are employed in the images. A fractal organization, as identified by straight lines with non-integer slopes in Fig. 8, represents images containing clusters of close neighboring colors as well as colors that are far apart. At the same time, a fractal structure with exponent D less than 3, indicates voids of all sizes with no colors for the three-dimensional histograms in the colorimetric cube. In this way, natural images appear to involve colors that are selected in a non-trivial self-similar fractal fashion over the colorimetric cube, with color

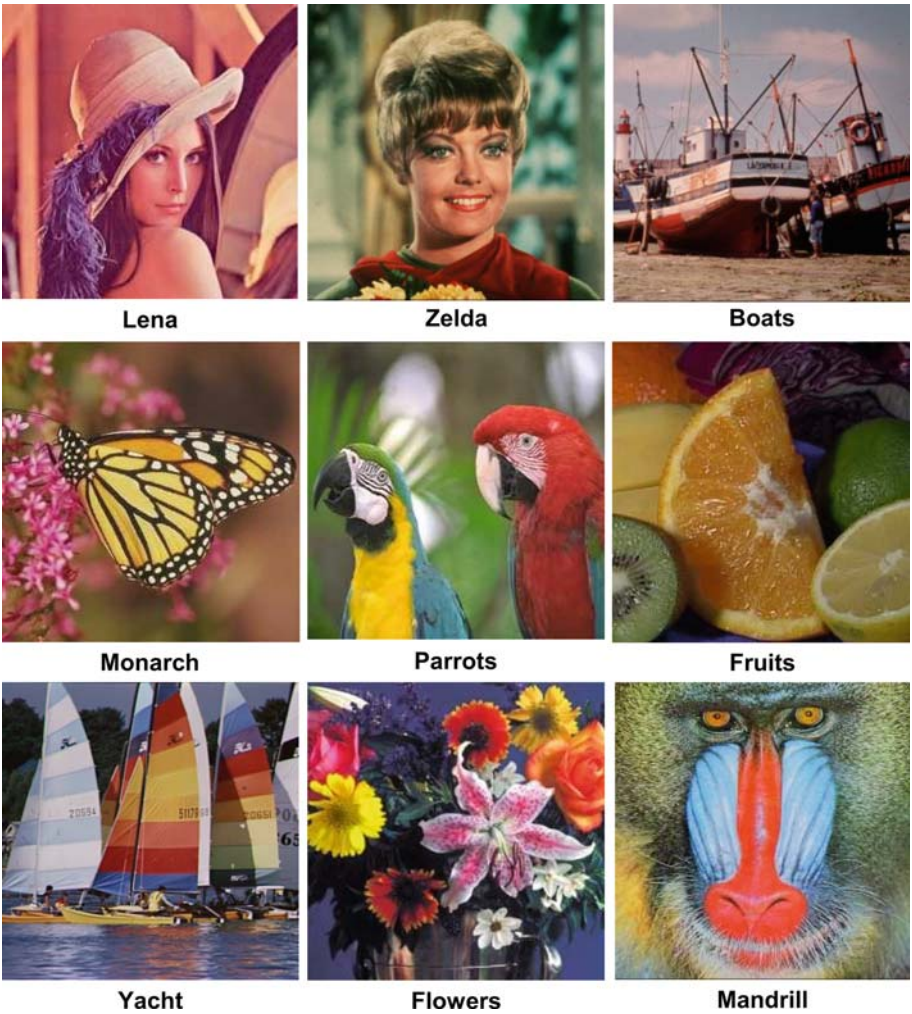

Fig. 6 Nine RGB color images with size 512 × 512 pixels, and $Q = 256$ levels

selected uniformly across many scales. Small scales are related to the many different shades and variations of some generic reference colors, large scales are related to the several largely distinct colors that frequently compose natural images. And these different colors are usually recruited in a self-similar way across scales, as manifested by Fig. 8.

The results of Fig. 8 characterize a fractal structure in the colorimetric organization of natural images by means of the box-counting method and what is known as the capacity dimension D (Maggi and Winterwerp 2004; Schroeder 1999). It is possible to confront this characterization with other recent approaches to the colorimetric organization of natural images (Chauveau et al. 2008; Chapeau-Blondeau et al. 2009). These approaches of Chauveau et al. (2008), Chapeau-Blondeau et al. (2009) perform a fractal characterization based on the evaluation of the correlation dimension of the three-dimensional color histogram. This evaluation relies on two distinct estimators in Chauveau et al. (2008) and in

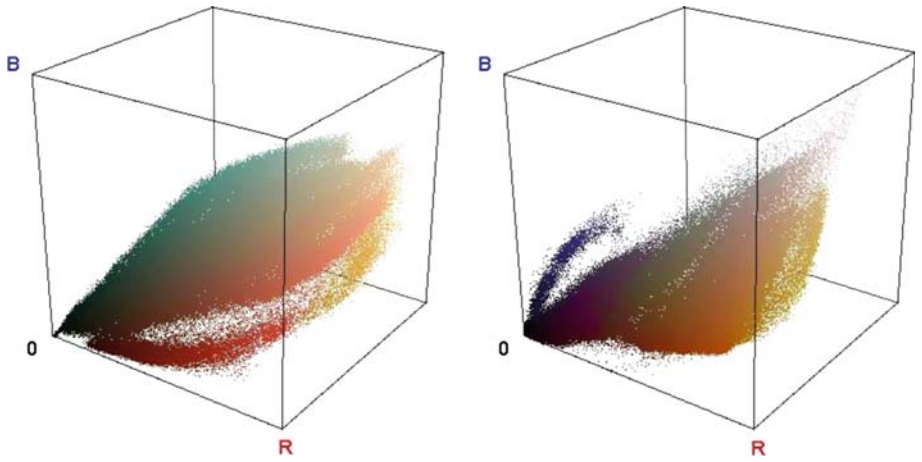

Fig. 7 Color histogram in the RGB colorimetric cube $[0, 255]^3$ for image "Zelda" (*left*) and image "Fruits" (*right*) from Fig. 6

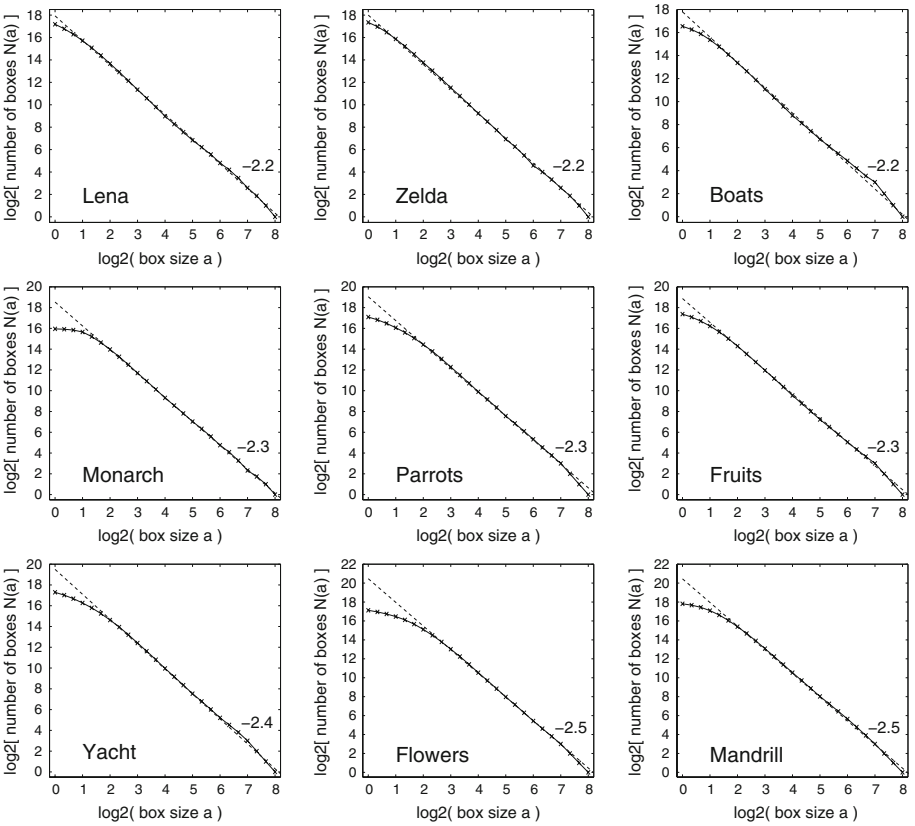

Fig. 8 Number $N(a)$ of covering boxes with size a to cover the three-dimensional histogram, for the nine RGB color images of Fig. 6. For each image, the *dotted line* shows the slope $-D$

Table 1 The capacity dimension $D = D_0$ evaluated by the box-counting method of Fig. 8, and the correlation dimension D_2 evaluated from the correlation integral as in Chapeau-Blondeau et al. (2009). The nine images of Fig. 8 are treated first, complemented by three other standard images not displayed in Fig. 6 but coming from Chapeau-Blondeau et al. (2009) or Chauveau et al. (2008)

Image	Capacity dim. $D = D_0$	Correlation dim. D_2
Lena	2.2	1.9
Zelda	2.2	2.1
Boats	2.2	1.8
Monarch	2.3	1.7
Parrots	2.3	1.8
Fruits	2.3	1.9
Yacht	2.4	1.8
Flowers	2.5	1.3
Mandrill	2.5	2.3
Goldhill	2.2	2.1
Car	2.3	1.5
Sailboat	2.3	1.7

Chapeau-Blondeau et al. (2009), developed for the correlation integral, as pioneered by Grassberger and Procaccia to characterize strange attractors of chaotic dynamics (Grassberger and Procaccia 1983). For the three-dimensional histogram from natural color images, we confront in Table 1, the capacity dimension $D = D_0$ evaluated by the box-counting method of Fig. 8, with the correlation dimension D_2 evaluated in Chapeau-Blondeau et al. (2009) from the correlation integral of Grassberger and Procaccia (1983). In Table 1, some of the values of D_2 are directly taken from Chapeau-Blondeau et al. (2009) while some others not given in Chapeau-Blondeau et al. (2009) have been computed here with the method of Chapeau-Blondeau et al. (2009). It is to be noted that these two characterizations by D_0 and D_2, constitute two distinct complementary points of view on the fractal properties. The capacity dimension D_0 and the correlation dimension D_2 are two important (and very often considered) instances in the infinite series of fractal dimensions which can be defined for fractal structures (Hentschel and Procaccia 1983; Schroeder 1999). As established already in Grassberger and Procaccia (1983), the capacity dimension D_0 and the correlation dimension D_2 are usually different and verify $D_0 \geq D_2$, as observed in Table 1.

In Table 1, both the capacity dimension and the correlation dimension assume non-integer values, and in this way they both manifest a fractal organization of the three-dimensional histogram of the color images. However, these two dimensions reflect different aspects of the fractal organization.

The results of Fig. 8 associated with the capacity dimension $D = D_0$ from the box-counting method, characterize, as we already mentioned, the support of the three-dimensional histogram. Equivalently, this measures which colors of the colorimetric cube are used and which are not used in the image. This support, according to Fig. 8, tends to display a fractal structure, with clusters and voids spanning many scales in a self-similar way. This is manifested in Fig. 8 by the linear scaling in log-log coordinates, with non-integer slopes defining the fractal dimension $D = D_0$ representing the capacity dimension or dimension of the support of the distribution. In other words, the capacity dimension characterizes the structure of the color palette employed by Nature to compose a given natural image. And Fig. 8 expresses that such a color palette tends to display a fractal organization, identified by a non-integer capacity dimension.

By contrast, the correlation dimension D_2 explored in Chauveau et al. (2008), Chapeau-Blondeau et al. (2009) and reproduced in Table 1, offers a more composite view. Through its mode of calculation as explained in Chauveau et al. (2008), Chapeau-Blondeau et al. (2009), the correlation dimension D_2 is affected by the color palette and by the populations of pixels distributing among these existing colors. This performs a joint characterization of both the support of the histogram and of the populations in the histogram. Equivalently, this measures simultaneously which colors are used in the histograms, and which populations of pixels distribute among these occupied colors. In this respect, it can be noted in Table 1 that, among the different images, there is more variability of the values found for the correlation dimension D_2 which evolve in the interval [1.5, 2.3], compared to the values found for the capacity dimension $D = D_0$ evolving in [2.2, 2.5]. This larger variability of D_2 is consistent with the fact that D_2 is affected by two properties of the histogram—the structure of its support (the color palette) and the populations of pixels filling these colors. Meanwhile, the capacity dimension $D = D_0$ is affected only by the support, and consistently experiences less variability across the images in Table 1.

Clearly, the characterization by the capacity and the correlation dimensions stand as two distinct, complementary, approaches to contribute to the analysis of the colorimetric organization of images. Their confrontation is realized for the first time here, thanks to the evaluation of the capacity dimension we perform. The correlation dimension D_2 points to a fractal organization for the way the pixels populate the occupied colorimetric cells of the histogram. The capacity dimension $D = D_0$ from Fig. 8 reveals that the occupied colorimetric cells alone, irrespective of their populations, display a fractal organization. These are two distinct fractal properties, which are both useful to characterize the complex colorimetric organization of natural images.

A consistent behavior of the capacity dimension can be observed when the box-counting procedure is applied to natural gray images coded as RGB colors images with three identical color components R = G = B. In this case, as shown in Fig. 9, the number of covering boxes is $N(a) \propto a^{-D}$ with $D = 1$, because the three-dimensional RGB histogram of the gray images is supported by the principal diagonal of the colorimetric cube, which is a one-dimensional manifold, much like in Fig. 3.

It is clear that a fractal dimension is a useful scalar index to summarize fractal properties in the three-dimensional histogram of the images. We have confronted several approaches for extracting a fractal dimension for the color histograms, by the box-counting method in Fig. 8 or via the correlation integral of Grassberger and Procaccia (1983) approached with two distinct estimators in Chauveau et al. (2008), Chapeau-Blondeau et al. (2009). The results of Fig. 8 estimate the capacity dimension $D = D_0$ by means of a simple linear fit. This is a straightforward approach which requires minimal hypothesis concerning the observed data, and as such it is very useful as a simple and direct reference. Other more sophisticated estimation procedures exist which require further hypothesis on the data, for instance estimators based on maximum likelihood formalism which require the specification of a probabilistic framework for assessing the probabilities of observing the data (Theiler 1990; Galka 2000). The Takens, or the binomial, or the Judd estimators are of this kind, as applied to the correlation dimension in Galka (2000), Theiler (1990). Here, the approach in Fig. 8 is directly based on counts on the actual observed data, with no probabilistic assumption required. It stands as a natural reference if, beyond, one wants to compare methods for extracting a fractal dimension from the graphs of Fig. 8. However, we want to emphasize that the graphs of Fig. 8 allow one to appreciate also the whole scaling behavior of the histogram in the colorimetric space, across the whole range of scales available for the images. The significance here goes beyond the mere extraction of a fractal dimension, which may possibly differ slightly with

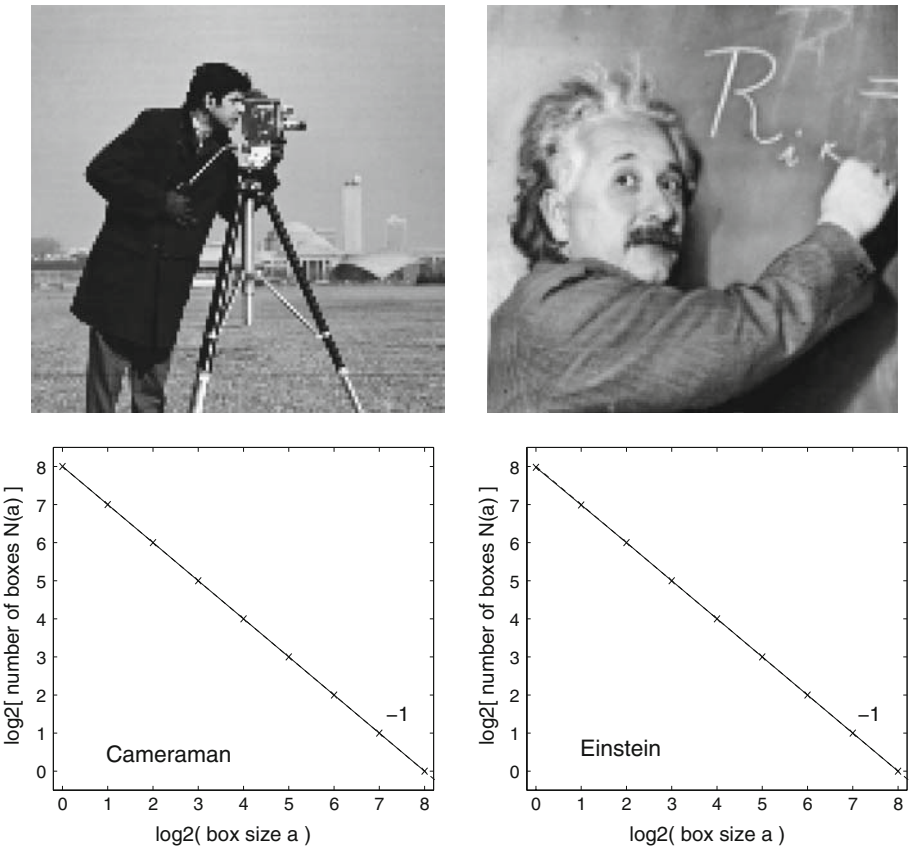

Fig. 9 Two gray-level images with size 512 × 512 pixels and $Q = 256$ levels, coded as RGB color images with three identical color components $R = G = B$; and corresponding number $N(a)$ of covering boxes with size a to cover their three-dimensional histogram

one method or another. Defining a fractal dimension usually involves a regular linear scaling behavior at small scales only, theoretically via a limit at scales going to zero. Here, the graphs of Fig. 8 reveal a regular scaling behavior linear almost over the whole range of scales (small and large) accessible for the histograms. It is this whole scaling behavior, as shown in Fig. 8, which is first of all significant concerning the structure of the colorimetric organization of the images.

5 Discussion

The characterization by the box-counting method performed in Sect. 4 indicates that the three-dimensional histograms from natural color images tend to display a support with a fractal structure. This complements the other recent characterization of Chauveau et al. (2008), Chapeau-Blondeau et al. (2009) showing a fractal organization also for the populations of pixels over the populated colors of the histograms. These results represent a first stage of exploration in this direction for characterizing the complex structure of images in

the colorimetric domain. They next should be complemented by examination of extended series of natural images, possibly with control on their typologies, in the direction which has been opened.

For natural images, such characterizations of fractal properties in their colorimetric organization complement other fractal properties previously established, through a gradual process with successive studies, in their spatial organization (Tolhurst et al. 1992; Ruderman and Bialek 1994; Ruderman 1997; Bex and Makous 2002; Hsiao and Millane 2005). The traditional methodologies for revealing spatial fractal properties in images usually rely on the frequency spectrum or on the autocorrelation function of the images. Power-law evolutions of such quantities are taken as the mark of a scale-invariant or fractal character (Schroeder 1999) in the images. Specific self-similar models, like the fractional Brownian motion, precisely endowed with power-law autocorrelation and spectrum, have been shown capable to provide relevant descriptions of the variations of intensities over natural images (Mandelbrot 1983; Pentland 1984; Keller et al. 1987; Potlapalli and Luo 1998; Kaplan 1999; Pesquet-Popescu and Lévy Véhel 2002). In such situations, the origin of the fractal self-similar behavior relates to the spatial organization of the features and details across the image. Application of fractal concepts to image compression (Jacquin 1992; Fisher 1995; Wohlberg and De Jager 1999; Truong et al. 2004; Faraoun and Boukelif 2005) has emerged in this context of spatial fractality in natural images. Also, this type of spatial characterization of fractal properties has been mostly applied to gray-level or one-component images. The approach we developed here is quite different since it specifically applies to RGB color images, and it offers a characterization of the image in the colorimetric domain as a complement to the spatial domain. The common aspect is the power-law scaling of relevant quantities, as in Fig. 8, which is in each case taken as the mark of a scale-invariant fractal organization. However, the scaling quantities are quite different to reveal spatial or colorimetric fractal properties. And while fractality in the spatial organization was previously known for natural images, fractality in the colorimetric organization as addressed here constitutes a novel direction of exploration.

For color images as considered here, the fractal dimensions resulting from such analyses of their three-dimensional histograms, stand as simple characteristic parameters, which can be helpful to various purposes such as image classification or indexing, or contribute to metrics for realistic synthesis of images (Gevers and Smeulders 1999; Batlle et al. 2000; Distasi et al. 2003; Lian 2008; Sharma 2003). Also, a fractal organization indicates clusters of occupied colorimetric cells exhibiting many sizes, over many scales, in the three-dimensional histograms. This is to be contrasted with simpler structures composed of a few clusters, with a few definite sizes, for the occupied colorimetric cells of the histograms. This may bear relevance to segmentation of color images based on pixel clustering from the color histogram. The presence of a fractal organization suggests that there is no such thing as a small number of well defined clusters that would emerge in the three-dimensional histograms, but on the contrary, many clusters and sub-clusters co-existing over many scales in a self-similar way.

Uncovering fractal structures also provides clues useful to developing models for natural images (Srivastava et al. 2003; Gousseau and Roueff 2007). This is an important task for many areas of image processing and computer vision. The fractal organization observable in the three-dimensional color histograms of natural images can have its origin in the spatial structures present in natural scenes, typically containing features and details spanning many scales. In this direction, the fractal colorimetric organization reported here for natural images, would share some common origin with the distinct fractal spatial organization previously reported for natural images (Tolhurst et al. 1992; Ruderman and Bialek 1994; Ruderman 1997; Hsiao and Millane 2005). Also, trichromacy for color representation is a coding modality inherent to the visual system. Fractal organization in the colorimetric

structure of natural images could reveal some coding principles implemented by the visual system itself (Field 1987, 1994; Olshausen and Field 2000). Fractal self-similar organization of the colors perceived in natural images, could represent some optimal way of distributing the contrast discrimination capabilities of the visual system across the colorimetric domain. In this way, the visual system would be equally capable of distinguishing small colorimetric contrasts of close colors as well as large contrasts of very different colors.

6 Conclusion

The present study has implemented a fractal characterization of the three-dimensional histogram from natural color images. The most prominent findings lie in the regular scaling behavior which is observed almost linear over the whole range of accessible scales, and with non-integer slope. This type of scaling identifies a fractal colorimetric organization which is characterized here with the capacity dimension. This remarkable linear scaling is persistent among the standard color images that were tested here, and it points to a highly structured organization of natural images in the colorimetric domain. The non-integer capacity dimension was observed to vary from one image to the other, yet in a rather narrow range, typically between 2.2 and 2.5. The capacity dimension has been confronted with the very recently measured correlation dimension which offers a different viewpoint on the color histograms, and both dimensions consistently confirm a fractal organization. Similar fractal approaches as addressed here for the three-dimensional histogram of color images, can be extended to multispectral images, to characterize the complex structure of their multidimensional histograms, contribute to assess their intrinsic dimensionality, and suggest efficient representations in reduced coordinate systems (Landgrebe 2002). All these aspects connected to fractal properties in images, and possibly relevant to many areas of image processing and artificial or natural vision, offer promising directions for further investigation.

Acknowledgments Julien Chauveau acknowledges support from *La Communauté d'Agglomération du Choletais*, France.

References

Batlle, J., Casalsb, A., Freixeneta, J., & Martía, J. (2000). A review on strategies for recognizing natural objects in colour images of outdoor scenes. *Image and Vision Computing, 18*, 515–530.

Bex, P. J., & Makous, W. (2002). Spatial frequency, phase, and the contrast of natural images. *Journal of the Optical Society of America A, 19*, 1096–1106.

Chapeau-Blondeau, F., Chauveau, J., Rousseau, D., & Richard, P. (2009). Fractal structure in the color distribution of natural images. *Chaos, Solitons & Fractals, 42*, 472–482.

Chauveau, J., Rousseau, D., & Chapeau-Blondeau, F. (2008). Pair correlation integral for fractal characterization of three-dimensional histograms from color images. In *Lecture notes in computer science*, (vol. LNCS 5099, pp. 200–208). Berlin: Springer.

Chen, Y. C., Ji, Z., & Hua, C. (2008). Spatial adaptive Bayesian wavelet threshold exploiting scale and space consistency. *Multidimensional Systems and Signal Processing, 19*, 157–170.

Distasi, R., Nappi, M., & Tucci, M. (2003). FIRE: Fractal indexing with robust extensions for image databases. *IEEE Transactions on Image Processing, 12*, 373–384.

Dong, D. W., & Atick, J. J. (1995). Statistics of natural time-varying images. *Network: Computation in Neural Systems, 6*, 345–358.

Faraoun, K. M., & Boukelif, A. (2005). Speeding up fractal image compression by genetic algorithms. *Multidimensional Systems and Signal Processing, 16*, 217–236.

Field, D. J. (1987). Relations between the statistics of natural images and the response properties of cortical cells. *Journal of the Optical Society of America A, 4*, 2379–2394.

Field, D. J. (1994). What is the goal of sensory coding? *Neural Computation, 6*, 559–601.
Fisher, Y. (1995). *Fractal image compression: Theory and applications*. Berlin: Springer.
Galka, A. (2000). *Topics in nonlinear time series analysis*. Singapore: World Scientific.
Gevers, T., & Smeulders, A. W. M. (1999). Color-based object recognition. *Pattern Recognition, 32*, 453–464.
Gousseau, Y., & Roueff, F. (2007). Modeling occlusion and scaling in natural images. *SIAM Journal of Multiscale Modeling and Simulation, 6*, 105–134.
Grassberger, P., & Procaccia, I. (1983). Characterization of strange attractors. *Physical Review Letters, 50*, 346–349.
Hentschel, H. G. E., & Procaccia, I. (1983). The infinite number of generalized dimensions of fractals and strange attractors. *Physica D, 8*, 435–444.
Hsiao, W. H., & Millane, R. P. (2005). Effects of occlusion, edges, and scaling on the power spectra of natural images. *Journal of the Optical Society of America A, 22*, 1789–1797.
Jacquin, A. E. (1992). Image coding based on a fractal theory of iterated contractive image transformation. *IEEE Transactions on Image Processing, 1*, 18–30.
Kaplan, L. M. (1999). Extended fractal analysis for texture classification and segmentation. *IEEE Transactions on Image Processing, 8*, 1572–1585.
Keller, J. M., Crownover, R. M., & Chen, R. Y. (1987). Characteristics of natural scenes related to the fractal dimension. *IEEE Transactions on Pattern Analysis and Machine Intelligence, 9*, 621–627.
Knill, D. C., Field, D., & Kersten, D. (1990). Human discrimination of fractal images. *Journal of the Optical Society of America A, 7*, 1113–1123.
Landgrebe, D. (2002). Hyperspectral image data analysis. *IEEE Signal Processing Magazine, 19*(1), 17–28.
Lian, S. (2008). Image authentication based on fractal features. *Fractals, 16*, 287–297.
Maggi, F., & Winterwerp, J. C. (2004). Method for computing the three-dimensional capacity dimension from two-dimensional projections of fractal aggregates. *Physical Review E*, 69(011405), 1–8.
Mandelbrot, B. B. (1983). *The fractal geometry of nature*. San Francisco: Freeman.
Olshausen, B. A., & Field, D. J. (2000). Vision and the coding of natural images. *American Scientist, 88*, 238–245.
Pentland, A. P. (1984). Fractal-based description of natural scenes. *IEEE Transactions on Pattern Analysis and Machine Intelligence, 6*, 661–674.
Pesquet-Popescu, B., & Lévy Véhel, J. (2002). Stochastic fractal models for image processing. *IEEE Signal Processing Magazine, 19*(5), 48–62.
Potlapalli, H., & Luo, R. C. (1998). Fractal-based classification of natural textures. *IEEE Transactions on Industrial Electronics, 45*, 142–150.
Ruderman, D. L. (1997). Origins of scaling in natural images. *Vision Research, 37*, 3385–3398.
Ruderman, D. L., & Bialek, W. (1994). Statistics of natural images: Scaling in the woods. *Physical Review Letters, 73*, 814–817.
Schroeder, M. (1999). *Fractals, chaos, power laws*. New York: Freeman.
Sharma, G. (Ed.). (2003). *Digital color imaging handbook*. Boca Raton: CRC Press.
Srivastava, A., Lee, A. B., Simoncelli, E. P., & Zhu, S. C. (2003). On advances in statistical modeling of natural images. *Journal of Mathematical Imaging and Vision, 18*, 17–33.
Theiler, J. (1990). Estimating fractal dimension. *Journal of the Optical Society of America A, 7*, 1055–1073.
Tolhurst, D. J., Tadmor, Y., & Chao, T. (1992). Amplitude spectra of natural images. *Ophthalmic and Physiological Optics, 12*, 229–232.
Truong, T. K., Kung, C. M., Jeng, J. H., & Hsieh, M. L. (2004). Fast fractal image compression using spatial correlation. *Chaos, Solitons & Fractals, 22*, 1071–1076.
Wohlberg, B., & De Jager, G. (1999). A review of the fractal image coding literature. *IEEE Transactions on Image Processing, 8*, 1716–1729.

Author Biographies

Julien Chauveau was born in 1981 in France. He received a Master degree in computing and information science in 2007 from the University of Angers, France. He is currently a Ph.D. student in the field of imaging and image processing at the University of Angers, France.

David Rousseau was born in 1973 in France. He received the Master degree in acoustics and signal processing from the *Institut de Recherche Coordination Acoustique et Musique* (IRCAM), Paris, France in 1996. He received, in 2004, the Ph.D. degree in nonlinear signal processing and stochastic resonance at the *Laboratoire d'Ingénierie des Systèmes Automatisés* (LISA), University of Angers where he is currently a *Maître de Conférences* of physics and information sciences.

François Chapeau-Blondeau was born in France in 1959. He received the Engineer Diploma from ESEO, Angers, France, in 1982, the Ph.D. degree in electrical engineering from University Pierre et Marie Curie, Paris 6, France, in 1987, and the *Habilitation* degree from the University of Angers, France, in 1994. In 1988, he was a research associate in the Department of Biophysics at the Mayo Clinic, Rochester, Minnesota, USA, working on biomedical ultrasonics. Since 1990, he has been with the University of Angers, France, where he is currently a professor of electronic and information sciences. His research interests include nonlinear systems, signal processing and imaging, and the interactions between physics and information sciences.